

# Non-linear Equalization in 112 Gb/s PONs Using Kolmogorov-Arnold Networks

Rodrigo Fischer,<sup>1,\*</sup> Patrick Matalla,<sup>2</sup> Sebastian Randel,<sup>2</sup> and Laurent Schmalen<sup>1</sup>

<sup>1</sup>Communications Engineering Lab (CEL), Karlsruhe Institute of Technology, 76131 Karlsruhe, Germany

<sup>2</sup>Institute of Photonics and Quantum Electronics (IPQ), Karlsruhe Institute of Technology, 76131 Karlsruhe, Germany

\*rodrigo.fischer@kit.edu

**Abstract:** We investigate Kolmogorov-Arnold networks (KANs) for non-linear equalization of 112 Gb/s PAM4 passive optical networks (PONs). Using pruning and extensive hyperparameter search, we outperform linear equalizers and convolutional neural networks at low computational complexity. © 2024 The Author(s)

## 1. Introduction

Passive optical networks (PONs) are optical access networks whose branching points consist entirely of passive elements, enabling a cost-effective implementation. They currently serve the majority of fiber broadband subscribers worldwide and an ongoing demand for bandwidth has led to recent standardization efforts that enabled 50 Gb/s line rate transmission [1], while the research community is investigating the technologies that will enable PONs beyond 100 Gb/s [2]. One possibility for achieving 100 Gb/s is the use of higher-order modulation formats in intensity-modulation and direct-detection (IM/DD) links. However, this comes at the cost of an increased signal-to-noise ratio (SNR) requirement and lower tolerance to non-linearities in the channel. In a PON, the semiconductor optical amplifiers (SOAs) used to improve the receiver sensitivity suffer from non-linear gain saturation and the electro-absorption modulator (EAM) responsible for modulating the intensity of the optical signal has a non-linear transfer function. Additionally, when using IM/DD, the chromatic dispersion (CD) corresponds to a non-linear channel effect. This motivates the use of non-linear equalizers at the receiver, specially with low computational complexity as costs in access networks are crucial. Previous works investigated gated recurrent unit (GRU)-based [3] equalizers as well as convolutional neural networks (CNNs)-based equalizers [4], [5].

In this paper, we investigate Kolmogorov-Arnold networks (KANs), a novel type of neural network architecture able to learn non-linear activation functions, as equalizers in PONs. They were first used in applications where the analysis of the learned activation functions was used to infer information about the training data, helping scientists discover symbolic formulas or identify important features in mathematical or physical problems [6]. KANs exhibit two main features that motivate their use as non-linear equalizers. First, smaller KANs can reportedly achieve comparable performance as traditional multi-layer perceptron (MLP) networks [6]. With this, we expect that the KAN non-linear activation functions can learn how to invert the non-linear channel more easily than MLP networks with ReLU activation functions. A second aspect is that there are a few simple strategies that we can use to obtain a multiplier-free implementation of the KAN.

In this work, we propose to use KANs as non-linear equalizers for PONs. We compare them with CNNs and equalizers based on finite impulse response (FIR) linear filters with the same computational complexity. We also highlight further characteristics of KANs that make them good candidates for non-linear low-complexity equalizers.

## 2. Kolmogorov-Arnold Networks (KANs)

In a conventional MLP network, a layer consists of a linear transform followed by a non-linear activation function, whose operation can be written as  $\mathbf{x}_{\ell+1} = \sigma_{\ell}(\mathbf{W}_{\ell}\mathbf{x}_{\ell} + \mathbf{b}_{\ell})$ , where  $\ell \in \{1, \dots, L\}$  is the layer index,  $\mathbf{W}_{\ell}$  is the weight matrix,  $\mathbf{b}_{\ell}$  is the bias vector,  $\mathbf{x}_{\ell}$  of size  $n_{\ell}$  are the inputs and outputs of the  $\ell$ -th and  $(\ell - 1)$ -th layers, and  $\sigma_{\ell}$  is the activation function, which can be chosen as ReLU, ELU, sigmoid, etc. [7], as depicted in Fig. 1 (a).

KANs propose a different layer operation, where the multiplications of the weights by the inputs are replaced by trainable 1D functions  $\phi_{\ell,i,j}(x_{\ell,j})$  [6], as shown in Fig. 1 (b), where each entry  $x_{\ell+1,i}$  of the output vector is obtained by computing  $x_{\ell+1,i} = \sum_{j \in \{1, \dots, n_{\ell}\}} \phi_{\ell,i,j}(x_{\ell,j})$ . This can be conveniently represented by a matrix-function notation  $\mathbf{x}_{\ell+1} = \Phi_{\ell}(\mathbf{x}_{\ell})$ , where  $\Phi_{\ell} = \{\phi_{\ell,i,j}\}$  contains the functions of layer  $\ell$ , which are applied to the entries of  $\mathbf{x}_{\ell}$  and summed in a matrix-vector multiplication fashion. With multiple layers, we have  $\text{KAN}(\mathbf{x}) = \Phi_L(\Phi_{L-1}(\dots\Phi_1(\mathbf{x})))$ , which enables the network to learn compositional relationships involving the data features.

A straightforward way to implement trainable 1D functions is to use B-splines [6]; we use linear B-splines centered at  $G$  grid points located at  $\{-4, \dots, 4 - t, 4\}$ , with  $t = 8/(G - 1)$ , which results in activation functions

of the form  $\phi_{\ell,i,j}(x) = \sum_{k=0}^{G-1} a_{\ell,i,j,k} \text{tri}(x + 4 - kt)$ , where  $a_{\ell,i,j,k} \in \mathbb{R}$  are the trainable parameters and  $\text{tri}(x)$  is the triangular function with unit height spanning from  $x = -t$  to  $x = t$ . This corresponds to a piece-wise linear function that interpolates the values  $a_{\ell,i,j,k}$  for  $k = 0, \dots, G - 1$  between the grid points. This can be implemented in hardware by first determining where the input  $x$  lies on the grid, followed by a single multiplication by a slope and a summation with an offset. The slopes and offsets can be stored in a lookup table (LUT) with  $G - 1$  entries.

### 3. Experimental Results and Discussion

We validate the novel KAN-based equalizer in a 112 Gb/s PON upstream transmission in the C-band, as depicted in Fig. 2. The setup is similar to the one reported in [4] but with some improvements regarding device losses and EAM operation point. At the optical network unit (ONU) side, we generate  $2^{19}$  symbols in a field-programmable gate array (FPGA) and use a Keysight USPA DAC3 signal converter to generate a 56 GBd non-return-to-zero (NRZ) 4-ary pulse amplitude modulation (PAM4) signal with a peak-to-peak voltage of 2 V. The signal modulates the optical light emitted by a distributed-feedback laser (DFB) laser at 1540 nm in a low-cost EAM modulator, which will distort the signal due to its non-linear transfer function (see Fig. 2, right). Afterwards, the signal is launched with an optical power of 4.1 dBm into a 2.2 km-long fiber, resulting in a total accumulated CD of about  $35.9 \text{ ps} \cdot \text{nm}^{-1}$  for a fiber-dependent CD coefficient of  $16.3 \text{ ps} \cdot \text{nm}^{-1} \cdot \text{km}^{-1}$ . Using a variable optical attenuator (VOA), we can adjust the received optical power (ROP). At the optical line terminal (OLT) receiver, an SOA with 3 nm optical bandpass filter is used due to the increased SNR requirements of PAM4 signals. Note that the SOA will add non-linear distortions caused by gain saturation, as shown in Fig. 2. The optical signal is detected using a 40 GHz-photodiode with conventional amplifier. Note, that further improvements in receiver sensitivity can be achieved using an avalanche photodiodes with transimpedance amplifier. The electrical signal is sampled using a 33 GHz-real-time oscilloscope at 80 GSa/s. In offline digital signal processing (DSP), the signal is resampled to twofold oversampling and synchronized using a blind feedforward clock recovery offering fast synchronization for PONs [8] before the KAN equalizer is applied.

For a ROP ranging from  $-30 \text{ dBm}$  to  $2 \text{ dBm}$  with a step size of 1 dBm, we collected 30 sequences per ROP with a length of  $2.8 \cdot 10^6$  PAM4 symbols at 2 samples per symbol (sps). One training iteration, where the network weights are updated, consisted of feeding 360 symbols in a convolution-manner through the equalizers for a total of 7600 iterations. Furthermore, we used the last 200 blocks of size 360 symbols of each sequence for testing, performed at the end of each training iteration. For all the models, we use the mean squared error (MSE) loss and a learning rate (LR) scheduler that multiplies the LR by a factor of  $\alpha_{\text{LR}} = 0.4$  when the training loss reaches a plateau. We also used  $L_1$  regularization of the weights with a factor of  $5 \cdot 10^{-3}$ , which enforces sparsity of the weights.

We considered 2-layer networks KAN-2 and CNN-2, as well as 1-layer network KAN-1, and FIR filters with different amount of taps. For the multi-layer networks, we perform layer-wise convolution of the inputs with  $C_{\text{out}}$  kernels (filters) of size  $K$  taps, moving the filter  $S$  samples at a time (stride). Table 1 shows an overview of the search space for the network architectures. Higher strides result in lower complexity per-symbol [4]. We also fix  $C_{\text{out}}$  in the last layer as  $1/\text{sps} \cdot \prod_{\ell=1}^L S_{\ell}$ , where  $S_{\ell}$  is the stride of the  $\ell$ -th layer, which guarantees that symbols enter and leave the equalizer at equal rate. Furthermore, we searched the LR over  $\{1, 1.77, 3.16, 5.62\} \cdot 10^{-3}$ . Pruning was performed by forcing the weights whose magnitude lies below a threshold w.r.t. the maximum weight magnitude for each layer to zero. For the KANs we used  $\sum_{k=0}^{G-1} |a_{\ell,i,j,k}|$  as a replacement for the magnitude of the weights. We used the thresholds  $\{0, 1.25, 2.5, 5, 10, 15, \dots, 95\} \%$  and we performed another round of training on the same sequences to adjust the remaining weights. In order to obtain the Pareto fronts, we used a subset of

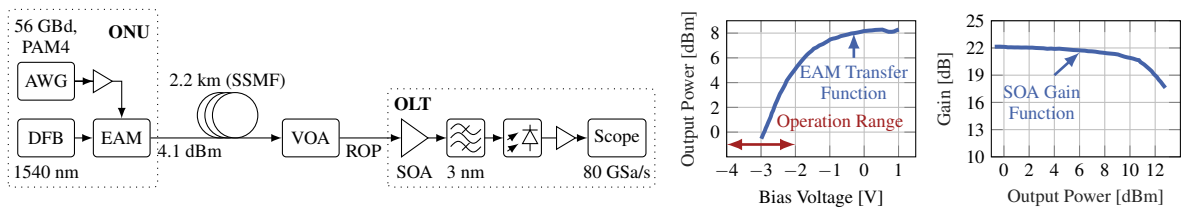


Fig. 2: Experimental setup for a 112 Gb/s (56 GBd, PAM4) PON upstream through a standard single-mode fiber (SSFM) in the C-band. In the right, the non-linear EAM transfer function and SOA gain function is shown.

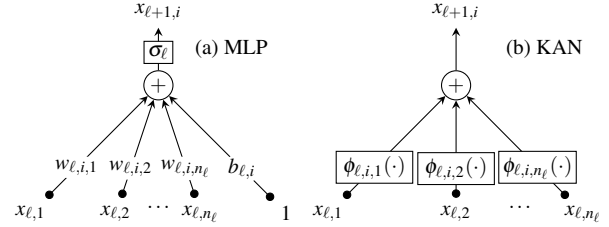
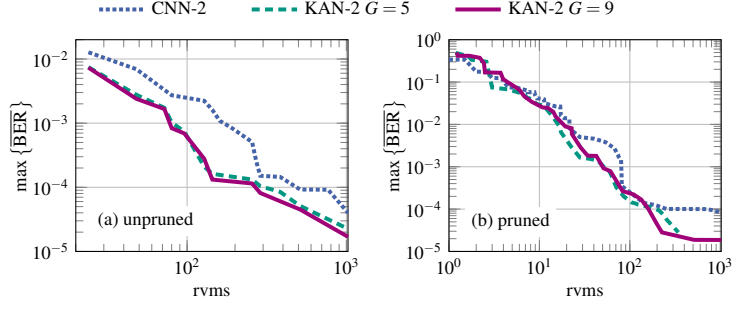


Fig. 1: Diagram of a single neuron in (a) a multi-layer perceptron (MLP) network and (b) a Kolmogorov-Arnold network (KAN) network, where boxes represent 1D functions.

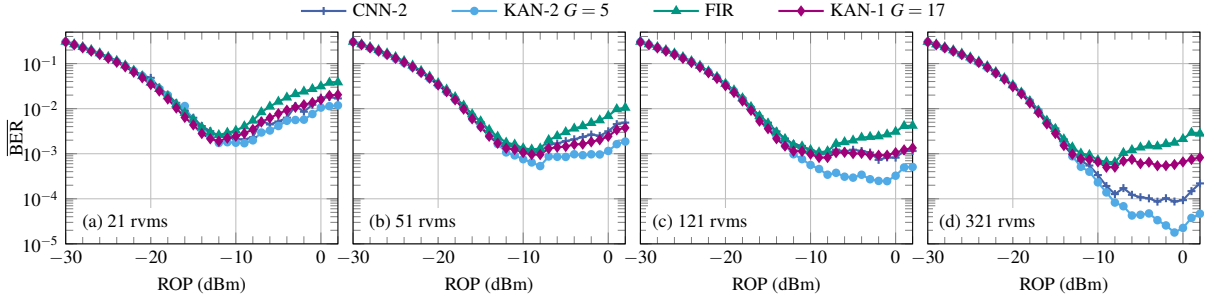
Table 1: Overview of the Search Space

Net	Layer	$C_{\text{out}}$	$K$	$S$	$G$
KAN-2/ CNN-2	Layer 1	$\{2, 4, 8\}$	$\{8, 32, 64\}$	$\{1, 2, 4\}$	$\{5, 9\}$
	Layer 2	$S_1 S_2 / 2$	$\{8, 32, 64\}$	$\{2, 4, 8\}$	$\{5, 9\}$
KAN-1/ FIR	Layer 1	1	$\{21, 51, 121, 321\}$	2	17/-

Fig. 3: Pareto fronts for unpruned (a) and pruned (b) networks at ROP =  $-2$  dBm and 2.2 km (C-band) considering the maximum over all training sequences of the mean BER taken at the last ten training iterations.

8 sequences at ROP =  $-2$  dBm and for each sequence we averaged the test bit error rate (BER) over the last 10 training iterations. To get a final metric, we took the maximum over the 8 sequences, which we denote by  $\max\{\text{BER}\}$ . By using the maximum metric, we hope to avoid choosing KAN and CNN architectures that may have a good median or mean performance, but that occasionally don't converge. We measure complexity in terms of the number of real-valued multiplications per symbol (rvms).

The Pareto fronts can be seen in Fig. 3 for the unpruned (a) and pruned (b) architectures. We observe a large gap between the CNNs and KANs for the unpruned networks and a smaller gap for the pruned networks, which seem to indicate that the KANs are more efficient in using the available weights than the CNNs, but once we remove the unused weights from the CNN, we have a Pareto front closer to that of the KANs. We show the performance of the models that lay on the pruned Pareto fronts at varying complexities on the entire measured ROP range in Fig. 4. The KAN-2 outperforms all the other models, but notably, the KAN-1 is able to have similar performance to the CNN-2 up until 121 rvms. Also, the gap between the FIR linear equalizers and the non-linear equalizers increase as the computational complexity increase.

Fig. 4: Mean  $\overline{\text{BER}}$  for a fiber length of 2.2 km (C-band) for models taken from the pruned Pareto curve with different complexities of 21 rvms (a), 51 rvms (b), 121 rvms (c) and 321 rvms (d).

#### 4. Conclusion

We showed that the novel KANs are able to outperform CNNs as equalizers in PONs at the same complexity, when compared in terms of rvms, while successfully compensating for the non-linearities in high ROPs also at low computational complexity.

**Acknowledgements:** This work has received funding from the European Research Council (ERC) under the European Union's Horizon 2020 research and innovation program (grant agreement No. 101001899).

#### References

1. R. Bonk *et al.*, "50G-PON: The first ITU-T higher-speed PON system," *IEEE Commun. Mag.*, vol. 60, no. 3, pp. 48–54, 2022.
2. R. Bonk *et al.*, "The road towards 100G and 200G-passive optical networks," in *Proc. ECOC*, 2024, p. W3D.4.
3. S. L. Murphy *et al.*, "High dynamic range 100G PON enabled by SOA preamplifier and recurrent neural networks," *J. Lightw. Technol.*, vol. 41, no. 11, pp. 3522–3532, 2023.
4. V. Lauinger *et al.*, "Fully-blind neural network based equalization for severe nonlinear distortions in 112 Gbit/s passive optical networks," in *Proc. OFC*, 2024, p. Th3J.5.
5. S. Li *et al.*, "CNN outperforms MMSE filtering at equal complexity while combating chromatic dispersion in PAM," in *Proc. ECOC*, 2024, p. Th1C.6.
6. Z. Liu *et al.*, "KAN: Kolmogorov-Arnold networks," *preprint arXiv:2404.19756*, 2024.
7. I. Goodfellow, Y. Bengio, and A. Courville, *Deep Learning*. MIT Press, 2016, ch. 6, <http://www.deeplearningbook.org>.
8. P. Matalla *et al.*, "Comparison of feedback and feedforward clock recoveries for ultra-fast synchronization in passive optical networks," in *Proc. OFC*, 2024, p. W2A.36.